Article

Introducing Krypton NMR Spectroscopy as a Probe of Void Space in Solids

Charlene F. Horton-Garcia, Galina E. Pavlovskaya, and Thomas Meersmann

J. Am. Chem. Soc., **2005**, 127 (6), 1958-1962• DOI: 10.1021/ja045636v • Publication Date (Web): 22 January 2005

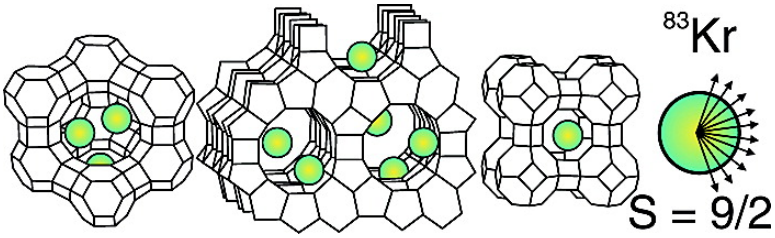

J|A|C|S
ARTICLES
Published on Web 01/22/2005

Introducing Krypton NMR Spectroscopy as a Probe of Void Space in Solids

Charlene F. Horton-Garcia, Galina E. Pavlovskaya, and Thomas Meersmann*

Contribution from the Department of Chemistry, Colorado State University, Fort Collins, Colorado 80523

Received July 20, 2004; E-mail: meer@lamar.colostate.edu

Abstract: A wealth of information about porous materials and their void spaces has been obtained from the chemical shift data in ^{129}Xe NMR spectroscopy during the past decades. In this contribution, the only NMR active, stable krypton isotope ^{83}Kr (spin $I = {}^{9}/_{2}$) is explored as a novel probe for porous materials. It is demonstrated that ^{83}Kr NMR spectroscopy of nanoporous or microporous materials is feasible and straightforward despite the low gyromagnetic ratio and low abundance of the ^{83}Kr isotope. The ^{83}Kr line width in most of the studied cases is quadrupolar dominated and field-strength independent. A significant exception was found in calcium-exchanged zeolites where the field dependence of the line width indicates a distribution of isotropic chemical shifts that may be caused by long-range disorder in the zeolite structure. The ^{83}Kr chemical shifts observed in the investigated materials display a somewhat different behavior than that of their ^{129}Xe counterparts and should provide a great resource for the verification or refinement of current ^{129}Xe chemical shift theory. In contrast to xenon, krypton with its smaller atomic radius has been demonstrated to easily penetrate the porous framework of NaA. Chemical shifts and line widths of ^{83}Kr are moderately dependent on small fluctuations in the krypton loading but differ strongly between some of the studied samples.

Introduction

The isotropic chemical shift observed in ^{129}Xe NMR spectroscopy has been extensively utilized during the past two decades as a probe for the size and loading of void space in solid host materials.[1−10] The anisotropy of the chemical shift (CSA) can be used to extract additional information such as local symmetry but is only observed in certain nanoporous solids.[11−13] Xenon's only other NMR active, stable isotope ^{131}Xe (21% natural abundance) has a nuclear electric quadrupole moment (spin $I = {}^{3}/_{2}$) and thus can provide information complementary to that obtained from ^{129}Xe NMR. The nuclear quadrupole moment is a sensor for local structure and symmetry because of its interaction with the electric field gradient (EFG) generated in the xenon electron shell by the local environment. An anisotropic environment can therefore lead to a quadrupolar splitting in the ^{131}Xe NMR spectrum as first demonstrated for xenon dissolved in anisotropic phases of liquid crystals.[14−17] Information about void space in porous materials can be extracted from coherent quadrupole interactions through multiple quantum filtered (MQF) experiments[18,19] or more directly through the observed line shape and through the second-order quadrupolar shift of the central transition.[20,21] The quadrupolar relaxation of ^{131}Xe also provides information about water adsorbed at the surface of the host structure,[19] an effect that was also used for contrast in magnetic resonance imaging (MRI).[22]

In this contribution we explore the only stable krypton isotope with nonzero spin and introduce ^{83}Kr NMR spectroscopy as a new probe for porous materials.[23] This isotope has a spin $I = {}^{9}/_{2}$ and a natural abundance of 11.5%. Its resonance frequency at 14.1 T is 23.1 MHz compared to 165 MHz for ^{129}Xe and 36.9 MHz for ^{131}Xe at the same field strength. The ^{83}Kr NMR

(1) Ito, T.; Fraissard, J. *J. Chem. Phys.* **1982**, *76*, 5225−5229.
(2) Ripmeester, J. A. *J. Am. Chem. Soc.* **1982**, *104*, 289−290.
(3) Dybowski, C.; Bansal, N.; Duncan, T. M. *Ann. Rev. Phys. Chem.* **1991**, *42*, 433−464.
(4) Jameson, C. J.; deDios, A. C. *J. Chem. Phys.* **1992**, *97*, 417−434.
(5) Dybowski, C. *J. Inclusion Phenom. Mol. Recognit. Chem.* **1995**, *21*, 113−136.
(6) Barrie, P. J.; Klinowski, J. *Prog. Nucl. Magn. Reson. Spectrosc.* **1992**, *24*, 91−108.
(7) Raftery, D.; Chmelka, B. F. *NMR* **1994**, *30*, 111−158.
(8) Ratcliffe, C. I. *Annu. Rep. NMR Spectrosc.* **1998**, *36*, 123−221.
(9) Bonardet, J. L.; Fraissard, J.; Gedeon, A.; Springuel-Huet, M. A. *Catal. Rev.—Sci. Eng.* **1999**, *41*, 115−225.
(10) Springuel-Huet, M. A.; Bonardet, J. L.; Gedeon, A.; Fraissard, J. *Magn. Reson. Chem.* **1999**, *37*, S1−S13.
(11) Springuel-Huet, M. A.; Fraissard, J. *Chem. Phys. Lett.* **1989**, *154*, 299−302.
(12) Ripmeester, J. A.; Ratcliffe, C. I. *J. Phys. Chem.* **1995**, *99*, 619−622.
(13) Jameson, C. J.; Jameson, A. K.; Gerald, R. E.; Lim, H. M. *J. Phys. Chem. B* **1997**, *101*, 8418−8437.
(14) Loewenstein, A.; Brenman, M. *Chem. Phys. Lett.* **1978**, *58*, 435−436.
(15) Diehl, P.; Jokisaari, J. *Chem. Phys. Lett.* **1990**, *165*, 389−391.
(16) Ingman, P.; Jokisaari, J.; Diehl, P. *J. Magn. Reson.* **1991**, *92*, 163−169.
(17) Jokisaari, J.; Ingman, P.; Lounila, J.; Pulkkinen, O.; Diehl, P.; Muenster, O. *Mol. Phys.* **1993**, *78*, 41−54.
(18) Meersmann, T.; Smith, S. A.; Bodenhausen, G. *Phys. Rev. Lett.* **1998**, *80*, 1398−1401.
(19) Meersmann, T.; Deschamps, M.; Bodenhausen, G. *J. Am. Chem. Soc.* **2001**, *123*, 941−945.
(20) Moudrakovski, I. L.; Ratcliffe, C. I.; Ripmeester, J. A. *J. Am. Chem. Soc.* **2001**, *123*, 2066−2067.
(21) Millot, Y.; Man, P. P.; Springuel-Huet, M. A.; Fraissard, J. *C. R. Acad. Sci., Ser. IIc: Chim.* **2001**, *4*, 815−818.
(22) Pavlovskaya, G.; Blue, A. K.; Gibbs, S. J.; Haake, M.; Cros, F.; Malier, L.; Meersmann, T. *J. Magn. Reson.* **1999**, *137*, 258−264.
(23) First presented at the 45th Experimental Nuclear Magnetic Resonance Conference, Asilomar, California April 2004.

10.1021/ja045636v CCC: $30.25

sensitivity is about 3.8% of the sensitivity obtained from thermally spin polarized ^{129}Xe and about 37% of that from ^{131}Xe at natural abundance. The quadrupole moment of ^{83}Kr is 0.26 $\times$ 10^{-28} m^2 and thus about twice that of ^{131}Xe (-0.12×10^{-28} m^2), but quadrupole interactions are usually smaller for krypton compared to xenon partially because of krypton's larger spin quantization and partially because of its smaller electron shell that is less polarizable. The smaller electron shell leads to smaller (internal) EFGs and smaller Sternheimer antishielding factors, thus causing reduced quadrupolar interactions. Early ^{83}Kr NMR research was focused on relaxation measurements in the gas, liquid, and solid phases.[24,25] Krypton relaxation and chemical shift measurements in various liquid solutions have also been reported.[26−28] The only previous material science NMR applications of krypton are studies of liquid crystalline phases, where anisotropic structure leads to a quadrupolar splitting in the ^{83}Kr NMR spectrum[16,17] and ^{129}Xe NMR chemical shift measurements in xenon−krypton gas mixtures within zeolites.[29,30] The quadrupolar splitting of ^{83}Kr found in liquid crystals is about 12 times smaller than those of ^{131}Xe under the same conditions. Similarly, the relaxation rates of ^{83}Kr in various solutions are about an order of magnitude slower than the corresponding ^{131}Xe rates.[31] Magnetic field induced quadrupolar splitting in gas and liquid phase ^{131}Xe at high magnetic field strengths[32−34] has not been observed with ^{83}Kr NMR.[35]

Results and Discussion

The ^{83}Kr NMR spectrum of krypton in various porous materials is shown in Figure 1 and displays relatively narrow line widths of 150−1100 Hz with most of the line widths around 400 Hz. For comparison, the ^{83}Kr NMR line widths in NaY zeolite are around 200−250 Hz, while the ^{131}Xe NMR line widths previously observed in the same material are around 1500 Hz.[20,21] The narrow lines reduce the sensitivity challenges and alleviate problems arising from acoustic ringing at the low Lamor frequency of krypton. Fast quadrupolar driven T_1 relaxation (on the order of a few milliseconds) shortens the experimental time, and spectra with reasonable signal-to-noise ratios can be recorded within a few hours or less depending on the porous material and the loading. The line widths of the ^{83}Kr NMR spectra recorded at two different field strengths of 14.1 and 9.4 T appear to be identical for each sample except for CaY (Si/Al = 5), CaX, and arguably for CaA. This is expected for a line shape that is caused either by coherent first-order quadrupolar interaction or by quadrupolar relaxation of systems with short correlation times. In contrast, chemical shift dispersion and chemical shift driven relaxation are the dominating factors for the (magnetic field strength dependent) line shape of ^{129}Xe in porous materials.

The ^{83}Kr line width decreases moderately (about 20%) with increasing external krypton pressure (ranging from 100 to 500 kPa) or with increasing krypton loading of the zeolites as shown in Figure 2. The pressure and loading dependence is relatively small compared to the range of line widths between the various zeolites studied, and therefore the results can be reliably reproduced for a given sample.

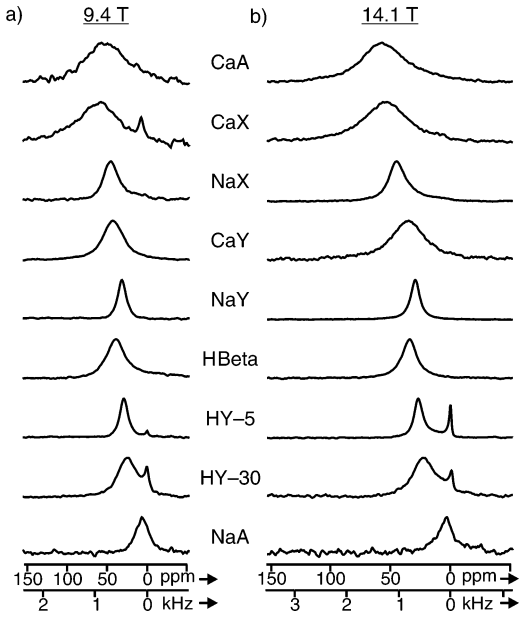

Figure 1. ^{83}Kr NMR spectra of a series of cation-exchanged zeolites as a function of field strength at (a) 9.4 T and (b) 14.1 T. All spectra were taken with an approximate value of 500 kPa of Kr gas and at 295 K. Both sets of spectra are depicted at the same ppm scale with the appropriate scaling in hertz also displayed. Spectra obtained are a product of signal averaging of between 3000 and 100 000 scans, depending on the signal-to-noise ratio obtained with a sample. HY-5 denotes HY (Si/Al = 5), and HY-30 denotes HY (Si/Al = 30).

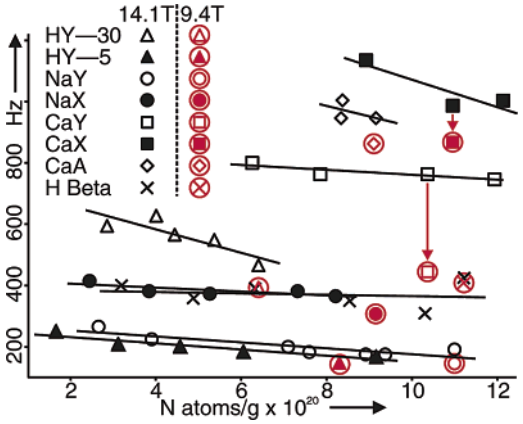

Figure 2. Line width dependence of the ^{83}Kr NMR signal on loading ([number N of Kr atoms/grams of zeolite material] $\times$ 10^{20}). Line widths are shown for 14.1 T spectra and 9.4 T spectra. Arrows are used to highlight the field-dependence of line width in the Ca-exchanged samples. Not displayed are data for NaA, since only one data point (at 14.1T, 284 Hz line width for 3.2 $\times$ 10^{20} atoms/g loading; at 9.4 T, 381 Hz line width for 3.7 $\times$ 10^{20} atoms/g loading) is available due to low signal intensity. HY-5 denotes HY (Si/Al = 5), and HY-30 denotes HY (Si/Al = 30). Linear fits to the data are only meant as a guide.

(24) Lurie, J.; Feldman, J. L.; Horton, G. K. *Phys. Rev.* **1966**, *150*, 180−185.
(25) Cowgill, D. F.; Norberg, R. E. *Phys. Rev. B* **1976**, *13*, 2773−2781.
(26) Mazitov, R. K.; Enikeev, K. M.; Ilyasov, A. V. *Z. Phys. Chem., Neue Folge* **1987**, *155*, 55−68.
(27) Enikeev, K. M.; Mazitov, R. K.; Ilyasov, A. V. *Z. Phys. Chem, Neue Folge* **1987**, *155*, 55−68.
(28) Luhmer, M.; Reisse, J. *Prog. Nucl. Magn. Reson. Spectrosc.* **1998**, *33*, 57−76.
(29) Jameson, A. K.; Jameson, C. J.; Dedios, A. C.; Oldfield, E.; Gerald, R. E.; Turner, G. L. *Solid State Nucl. Magn. Reson.* **1995**, *4*, 1−12.
(30) Jameson, C. J.; Jameson, A. K.; Lim, H. M. *J. Chem. Phys.* **1997**, *107*, 4364−4372.
(31) Jokisaari, J. *Prog. Nucl. Magn. Reson. Spectrosc.* **1994**, *26*, 1−26.
(32) Meersmann, T.; Haake, M. *Phys. Rev. Lett.* **1998**, *81*, 1211−1214.
(33) Salsbury, F. R., Jr.; Harris, R. A. *J. Chem. Phys.* **1998**, *109*, 8338−8341.
(34) Vaara, J.; Pyykko, P. *Phys. Rev. Lett.* **2001**, *86*, 3268−3271.
(35) No splitting was observed for gas-phase krypton-83 at 100 kPa pressure and at 16.92 T magnetic field strength at the NHMFL, Tallahassee, FL by one of us (TM).

Surprisingly, the ^{83}Kr line width in the calcium samples decreases as the magnetic field strength decreases from 14.1 to 9.4 T (Figures 1 and 2). Since CSA dispersion or CSA driven relaxation are unlikely to be dominant over quadrupolar broadening mechanisms, this field dependence may be caused by an isotropic chemical shift distribution within the sample. This effect is only apparent in the Ca-exchanged samples that have a higher degree of distortion in the framework caused by the calcium ion occupying site I (this site is more preferential for Ca^{2+} than Na^{+}) and thus distorting the faujasite framework at the double six-ring.[36,37] This leads to greater long-range disorder in the framework, as well as a more pronounced difference in the placement of Ca^{2+} cations in different supercages. Long-range disorder can cause an isotropic chemical shift dispersion (and therefore a field dependent line width) only if the length scale of the disorder exceeds the displacement that krypton atoms experience through diffusion at time scales on the order of the transverse relaxation time. Note that the Ca-exchanged samples have been produced through ion exchange from the corresponding Na^{+} zeolite crystallites that do not display the field dependence of the ^{83}Kr NMR line width (see Figures 1 and 2). All Ca-exchanged samples display line widths that are considerately broader (727−966 Hz) than the line widths of sodium and hydrogen containing zeolites except for NaX. The larger line broadening witnessed for NaX in contrast to NaY (Si/Al = 5) may be a result of the presence of the higher number of cations in the supercage of NaX. While NaX has sites II and III filled (both in the supercage), NaY (with its higher degree of dealumination) does not have as many of the sites III occupied due to the decreased number of cations (the cation number will mirror that of aluminum in the structure)[36] thus greatly reducing the number of cations able to interact with the guest krypton atoms. HBeta, a channeled structure, is found to have a relatively narrow line width of 400 Hz at 540 kPa, which is unexpected for a channeled structure where one would imagine that the line width would be greatly widened by anisotropy. However, HBeta has three intersecting orthogonal channel systems, and krypton atoms that are not restricted to 1-D movement will experience an environment that is less restricted than the surface of a single channel.

The NMR resonance shift data of krypton inside nanoporous materials reported in this contribution is the first of its kind for any porous material (see Figure 3). In analogy to the line width, the loading (and external pressure) dependence of the ^{83}Kr resonance shift is often smaller than the variation of shifts between various samples. This fact makes ^{83}Kr NMR a relatively reliable technique for practical purposes since changes in loading caused by small fluctuations in temperature or external gas pressure will not cause substantial errors in the line width and observed shift. Note, however, that the total chemical shift range of ^{83}Kr NMR for the data presented here is only about 1.2 kHz at 14.1 T field strength. The small shift range leads to substantially larger uncertainties compared to ^{129}Xe chemical shift data that would display a range of about 30 kHz at the same field strength. Nevertheless, it is worthwhile to address the krypton chemical shift in the context of previous xenon measurements.

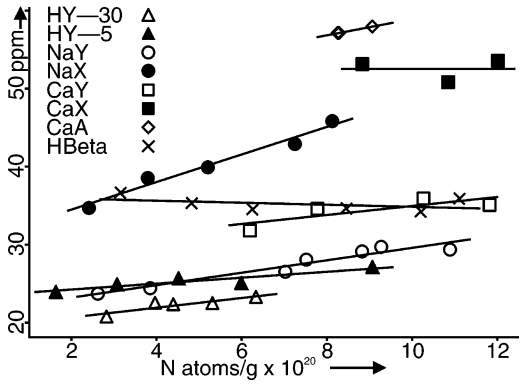

Figure 3. Chemical shift of the ^{83}Kr NMR signal (at 14.1 T) verses loading ([number N of Kr atoms/grams of zeolite material] $\times$ 10^{20}). NaA, with only one data point (3 ppm for 3.2 $\times$ 10^{20} atoms/g loading), has been omitted. HY-5 denotes HY (Si/Al = 5), and HY-30 denotes HY (Si/Al = 30). Slopes (ppm/[N atoms/g $\times$ 10^{20}]), and intercepts (ppm) for the linear fits for samples with more than three data points are as follows: HY (Si/Al = 30), 0.6, 19.3; HY(Si/Al = 5), 0.4, 23.3; NaY (Si/Al = 5), 0.8, 21.4; NaX, 1.7, 30.7; CaY (Si/Al = 5), 0.6, 28.9. The linear fit for HBeta (slope, −0.1; intercept, 35.8) is only meant as a guide, as theory does not predict a linear fit for this sample (see discussion in text).

The observed krypton chemical shift values in this work fall between 3 and 57 ppm. The lowest shift is observed in NaA, while the highest shifts are observed in the Ca-exchanged zeolites. All Ca-exchanged samples have high chemical shift values of 35−57 ppm, and no other sample approaches these values except for NaX (45 ppm at 500 kPa). A great deal of experimental and theoretical research on the xenon chemical shift in zeolites has been carried out in the past.[1−3,6,8,13] Fraissard and co-workers[9,10] have characterized the xenon chemical shift δ_{obs} in porous host structures as originating from various interactions:

$$\delta_{obs} = \delta_{ref} + \delta_{surf} + \delta_{gas}(\rho_{gas}) + \delta_{SAS}(\rho_{gas}) + \delta_{E} + \delta_{M} \quad (1)$$

where δ_{ref} is the reference shift and δ_{surf} is the shift that arises from the interactions of the xenon atom with the host structure that are averaged over various surface sites that are visited by the noble gas atom within its T_2 limited coherence lifetime. The chemical shift arising from Xe−Xe interactions δ_{gas} is dependent on the loading ρ_{gas} and in the most general case is given by an expansion in powers of the gas loading. At extrapolated zero xenon loading δ_{gas} will be zero and the shift term δ_{surf} is the remaining observed chemical shift if the contribution from the last three terms in eq 1 can be neglected. In this case, δ_{surf} is obtained from the zero intercepts of the fits of the loading dependent chemical shift data. The remaining terms in eq 1 are namely the chemical shift term δ_{SAS} caused by strong adsorption sites, the chemical shift term δ_{E} caused by electric charges in the zeolite pores, and the shift term δ_{M} caused by paramagnetic contributions in the material. It is reasonable to assume that eq 1 can also be used for the krypton chemical shift, but comparison of Figure 3 to previous xenon data shows some interesting differences. The experimental data for xenon-129 in NaY and HY zeolites show a convincing linear dependence with the loading[1] where the slopes and intercepts are identical for the zeolites with various silicon-to-aluminum ratios. The krypton chemical shift data in Figure 3 for HY (Si/Al = 5), HY (Si/Al = 30), and NaY (Si/Al = 5) also appear to follow a linear loading dependence with somewhat different slopes and inter-

(36) Smith, J. V. *Adv. Chem. Ser.* **1971**, 171−200.
(37) Vitale, G.; Bull, L. M.; Morris, R. E.; Cheetham, A. K.; Toby, B. H.; Coe, C. G.; Macdougall, J. E. *J. Phys. Chem.* **1995**, *99*, 16087−16092.

cepts for the three materials. More data, preferably obtained from a larger krypton loading range, will be needed to confirm the observed differences between the three materials. However, even considering the limitation arising from the limited chemical shift range and the small number of data points, it can be concluded that the slope and intercept for the NaX data in Figure 3 very clearly deviate from that for the HY (Si/Al = 5), HY (Si/Al = 30), and NaY (Si/Al = 5) zeolites (also see Figure 1). This is unexpected from previous xenon NMR and will need more investigation in future work. The ^{83}Kr chemical shifts for the HBeta zeolite display a slight negative slope if a linear fit is attempted. Fraisard and co-workers have pointed out that a linear fit (i.e., $\delta_{gas}(\rho_{gas}) = \delta_{gas}{\cdot}\rho_{gas}$) as a first-order approximation is applicable only for materials with large spherical cages where Xe−Xe collisions are isotropically distributed. An increasing, nonlinear slope can be observed in narrow channel structures with anisotropically distributed Xe−Xe collisions. This may be the case for krypton in the channel structure of HBeta, although the narrow line width (see discussion above) indicates otherwise and negative slopes are not expected from this effect in the first place. An explanation for the observed negative slope of the krypton chemical shift could be perhaps the presence of strong adsorption sites that can cause negative slopes for the chemical shift data at low loadings.

Equation 1 is valid for a spin $I = {}^1/_2$ noble gas, but another term needs to be considered for systems that possess a nuclear quadrupole moment. The observed ^{83}Kr NMR shift may in principle also be influenced by a second-order quadrupolar contribution. Previously obtained second-order shifts in ^{131}Xe NMR for NaY have been found to be about 5 ppm by comparison to ^{129}Xe NMR.[21] Thus far, no evidence for the presence of a second-order quadrupolar shift term was found by comparing the experimental ^{83}Kr chemical shift values and line widths at 9.4 and 14.1 T field strength. Unfortunately, the chemical shift data at 9.4 T display a relatively large uncertainty due to the limited shift range of only 900 Hz at this field strength, and the comparison remains inconclusive. Even if its quadrupole interactions are generally smaller than those for ^{131}Xe, the ^{83}Kr second-order shifts may still be significant on the (relative) ppm scale. At the very least, this effect will need to be considered for any explanation of the strong downfield shift of the krypton resonance in NaX compared to NaY. Since there is no stable spin $I = {}^1/_2$ krypton isotope, this will need to be explored by comparison with measurements at higher field strengths where second-order contributions will be diminished.

Equation 1 is useful to gain a physical picture of the interactions that drive the xenon chemical shift, but it does not assist in the theoretical calculation and prediction of the chemical shift. Enormous progress in the theoretical calculations of xenon chemical shift has been made using grand canonical Monte Carlo simulations[38−41] by Jameson and co-workers. It has also been pointed out that eq 1 is somewhat flawed in that the electric contribution, δ_E, to the chemical shift is generally rather small[42,43] and that δ_{surf} is not independent of the xenon density

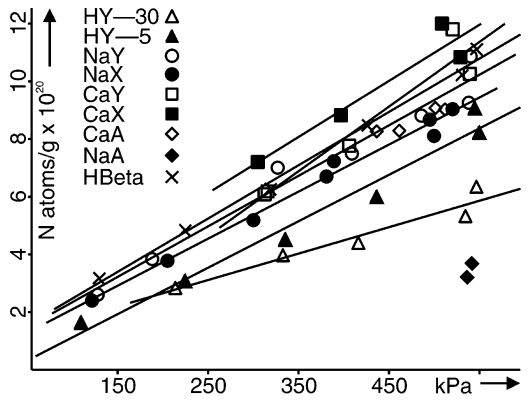

Figure 4. Adsorption isotherms of krypton in a series of cation-exchanged zeolites. HY-5 denotes HY (Si/Al = 5), and HY-30 denotes HY (Si/Al = 30). Linear fits to the data are only meant as a guide.

ρ_{gas}, at least in the case of NaA zeolite.[38,39] Furthermore, using a nonlinear dependence of δ_{gas} on the xenon density ρ_{gas} has been demonstrated even for NaX and NaY zeolites.[13] Clearly, simulations will be helpful to understand the krypton chemical shift data. Vice versa, the krypton data may be useful for the verification or refinement of current theory and may therefore lead to a better understanding of the xenon chemical shift behavior.

Another novelty of ^{83}Kr NMR is that a signal is easily observed in a NaA sample (cage opening 4 Å diameter) filled at room temperature and 500-kPa noble gas pressure. This is in stark contrast to xenon which can only be seen in NaA under much more extreme conditions and can be explained by the different atomic diameters, i.e., 3.9 Å for krypton and 4.4 Å for xenon. Previously this result was indirectly demonstrated through ^{129}Xe NMR studies of mixtures of xenon and krypton gases in NaA.[29,30] An important characteristic of the krypton signal in NaA is its low chemical shift of 3 ppm, while the next lowest chemical shift value is 23 ppm for HY (Si/Al = 30). Note that the lower signal intensity of krypton in NaA is a result of the lower loading of krypton in this zeolite as compared to the others studied, as shown in Figure 4.

In some materials, a strongly asymmetric local environment seems to disguise the ^{83}Kr NMR signal through very strong quadrupolar broadening. For instance, no signal was obtained in Ag-exchanged mordenite despite the fact that ^{129}Xe NMR has been successfully performed on mordenite samples.[44]

Conclusion

In summary, ^{83}Kr NMR spectroscopy provides promising information about void space in solid materials that is complimentary to ^{129}Xe NMR and ^{131}Xe NMR data. It is demonstrated that ^{83}Kr NMR spectroscopy of nanoporous or microporous materials is feasible even for routine applications at "medium" magnetic field strengths (i.e., 9.4 T or higher) despite the low gyromagnetic ratio and low abundance of the ^{83}Kr isotope. The relatively narrow line widths (i.e., 150−1100 Hz) make the observation of the ^{83}Kr signal and the suppression of acoustic ringing straightforward. The line shape and the observed chemical shift of the ^{83}Kr signal are only moderately dependent on small fluctuations in the krypton loading. This makes ^{83}Kr

(38) Jameson, C. J.; Jameson, A. K.; Baello, B. I.; Lim, H. M. *J. Chem. Phys.* **1994**, *100*, 5965−5976.
(39) Jameson, C. J.; Jameson, A. K.; Lim, H. M.; Baello, B. I. *J. Chem. Phys.* **1994**, *100*, 5977−5987.
(40) Jameson, C. J.; Jameson, A. K.; Gerald, R. E.; Lim, H. M. *J. Chem. Phys.* **1995**, *103*, 8811−8820.
(41) Jameson, C. J.; Jameson, A. K.; Lim, H. M. *J. Chem. Phys.* **1996**, *104*, 1709−1728.
(42) Adrian, F. J. *Phys. Rev. A* **1964**, *136*, A980-&.
(43) Bishop, D. M.; Cybulski, S. M. *J. Magn. Reson. Ser. A* **1994**, *107*, 99−101.
(44) Moudrakovski, I. L.; Ratcliffe, C. I.; Ripmeester, J. A. *Stud. Surf. Sci. Catal.* **1995**, *97*, 243−250.

NMR a relatively reliable technique despite the disadvantage arising from the small chemical shift range on the absolute frequency scale. The ^{83}Kr line width in most of the studied cases is quadrupolar dominated and field-strength independent. A significant exception was found in calcium-exchanged zeolites where the field dependence of the line width indicates a distribution of isotropic chemical shifts that may be caused by long-range disorder in the structure of the host material. Comparison between the observed ^{83}Kr chemical shifts in the various materials reveals the differences from their ^{129}Xe counterparts. ^{83}Kr chemical shifts should provide a great resource for the verification or refinement of current ^{129}Xe chemical shift theory; however, the role of second-order quadrupolar contributions to the observed shift needs to be investigated. Although medium magnetic field strengths lead to acceptable signal intensities, future ^{83}Kr NMR studies at very high magnetic fields are needed to obtain clues concerning second-order quadrupolar shift contributions and to investigate the field dependent line shapes. It is also advisable to collect more chemical shift data over a wider krypton loading range preferably at very high magnetic fields. Last, but not least, krypton in contrast to xenon readily enters the porous framework of NaA and thus provides a probe for some materials that do not easily allow xenon adsorption.

Experimental Section

Isotherms for krypton adsorption on a series of zeolites were performed between 100 and 550 kPa, at roughly 100 kPa intervals, and are shown in Figure 4. NaX was obtained from Sigma, NaA and CaA were obtained from Matheson, Coleman, and Bell, while NaY (Si/Al = 5), HBeta, HY (Si/Al = 5), and HY (Si/Al = 30) were obtained from Zeolyst International. The CaY (Si/Al = 5) and CaX samples were produced through ion exchange from NaY (Si/Al = 5) and NaX, respectively, using standard batch aqueous ion exchange techniques.[37] All samples were dehydrated 15−20 h on a vacuum at around 1 Pa and a temperature of 673 K with the exception of HBeta that was dehydrated at 473 K to prevent structural changes. Samples were then filled with a known amount of krypton gas, and loading was measured through the change in pressure after approximately 5 min at a temperature of 295 K. Samples were run at 295 K on both 14.1 and 9.4 T Chemagnetics NMR spectrometers with straightforward spin−echo sequences using 1-s pulse delays and echo times that are much shorter (i.e., 100 μs) than the presumed quadrupolar interactions. Spectra shown were obtained with a maximal signal averaging of 100 000 scans. The reference signal of ^{83}Kr is taken as that of krypton gas at 500 kPa.

Acknowledgment. This material is based upon work supported in parts by the National Science Foundation under Grant No.: CHE-0135082. Acknowledgment is made to the donors of the American Chemical Society Petroleum Research Fund, for partial support of this research under Grant No. ACS PRF 40625-AC. We also would like to thank Professor Dr. Gary Maciel for generously granting substantial access to a 600 MHz Chemagnetics Infinity spectrometer.

JA045636V